doi:10.1093/brain/awn113 *Brain* (2008), **131**, 1831–1844

Paroxysmal exercise-induced dyskinesia and epilepsy is due to mutations in *SLC2A1*, encoding the glucose transporter GLUT1

Arvid Suls,[1,2,3] Peter Dedeken,[4] Karolien Goffin,[5] Hilde Van Esch,[6] Patrick Dupont,[5] David Cassiman,[7] Judith Kempfle,[8,9] Thomas V. Wuttke,[8,9] Yvonne Weber,[8] Holger Lerche,[8,9] Zaid Afawi,[10] Wim Vandenberghe,[4] Amos D. Korczyn,[11] Samuel F. Berkovic,[12] Dana Ekstein,[13] Sara Kivity,[14] Philippe Ryvlin,[15] Lieve R. F. Claes,[1,2,3] Liesbet Deprez,[1,2,3] Snezana Maljevic,[8,9] Alberto Vargas,[8,9] Tine Van Dyck,[1,2,3] Dirk Goossens,[3,16] Jurgen Del-Favero,[3,16] Koen Van Laere,[5] Peter De Jonghe[1,2,3,17] and Wim Van Paesschen[4]

[1]Neurogenetics Group, VIB Department of Molecular Genetics, [2]Laboratory of Neurogenetics, Institute Born-Bunge, [3]University of Antwerp, Antwerpen, [4]Department of Neurology, [5]Division of Nuclear Medicine, [6]Center for Human Genetics, [7]Metabolic Center, University Hospital Gasthuisberg, Katholieke Universiteit Leuven, Leuven, Belgium, [8]Neurological Clinic, [9]Institute of Applied Physiology, University of Ulm, Germany, [10]Department of Neurology, Tel Aviv Sourasky Medical Center, [11]Sieratzki Chair of Neurology, Tel Aviv University, Jerusalem, Israel, [12]Department of Medicine, University of Melbourne (Austin Health), Heidelberg West, Australia, [13]Department of Neurology, Hadassah Ein Kerem University Medical Center, Jerusalem, Israel, [14]Epilepsy Unit, Schneider Children's Medical Center of Israel, Petach Tikvah, Israel, [15]Department of Functional Neurology and Epileptology, CTRS-INSERM IDEE, INSERM U821, Hospices Civils de Lyon and Université Claude Bernard Lyon1, Lyon, France, [16]VIB Department of Molecular Genetics, Applied Molecular Genomics Group and [17]Division of Neurology, University Hospital of Antwerp, Antwerpen, Belgium

Correspondence to: Prof. Dr Wim Van Paesschen, Department of Neurology, University Hospital Gasthuisberg, Katholieke Universiteit Leuven, Herestraat 49, BE-3000 Leuven, Belgium
E-mail: wim.vanpaesschen@uz.kuleuven.ac.be

Paroxysmal exercise-induced dyskinesia (PED) can occur in isolation or in association with epilepsy, but the genetic causes and pathophysiological mechanisms are still poorly understood. We performed a clinical evaluation and genetic analysis in a five-generation family with co-occurrence of PED and epilepsy ($n = 39$), suggesting that this combination represents a clinical entity. Based on a whole genome linkage analysis we screened *SLC2A1*, encoding the glucose transporter of the blood-brain-barrier, GLUT1 and identified heterozygous missense and frameshift mutations segregating in this and three other nuclear families with a similar phenotype. PED was characterized by choreoathetosis, dystonia or both, affecting mainly the legs. Predominant epileptic seizure types were primary generalized. A median CSF/blood glucose ratio of 0.52 (normal >0.60) in the patients and a reduced glucose uptake by mutated transporters compared with the wild-type as determined in *Xenopus* oocytes confirmed a pathogenic role of these mutations. Functional imaging studies implicated alterations in glucose metabolism in the corticostriate pathways in the pathophysiology of PED and in the frontal lobe cortex in the pathophysiology of epileptic seizures. Three patients were successfully treated with a ketogenic diet. In conclusion, co-occurring PED and epilepsy can be due to autosomal dominant heterozygous *SLC2A1* mutations, expanding the phenotypic spectrum associated with GLUT1 deficiency and providing a potential new treatment option for this clinical syndrome.

Keywords: GLUT1; paroxysmal dyskinesia; exercise-induced; GLUT1 deficiency syndrome; ketogenic diet

Abbreviations: AED = antiepileptic drugs; FDG = 2-[^{18}F]Fluoro-2-deoxy-D-glucose; GLUT1 = facilitative glucose transporter type 1; GLUT1 DS = GLUT1 deficiency syndrome; LOD = logarithms of odds; MNI = Montreal Neurological Institute; OMG = 3-O-methyl-D-glucose; PED = paroxysmal exercise-induced dyskinesias; PHD = paroxysmal hypnogenic dyskinesias; PKD = paroxysmal kinesigenic dyskinesias; PNKD = paroxysmal non-kinesigenic dyskinesias; SPM = statistical parametric mapping

Received January 31, 2008. Revised April 4, 2008. Accepted May 12, 2008. Advance Access publication June 26, 2008

Introduction

Paroxysmal dyskinesias are characterized by transient abnormal, involuntary movement, such as choreoathetosis and dystonia, but unlike the epilepsies they do not evolve into tonic–clonic seizures, and are not associated with epileptiform discharges and alterations in consciousness (Berkovic, 2000). Broadly, the paroxysmal dyskinesias can be subdivided into four subgroups based upon precipitating factors: paroxysmal kinesigenic dyskinesia (PKD), paroxysmal non-kinesigenic dyskinesia (PNKD), paroxysmal exercise-induced dyskinesia (PED) and paroxysmal hypnogenic dyskinesia (PHD) (Demirkiran and Jankovic, 1995). The association between paroxysmal dyskinesias and other neurological disorders, like epilepsy or ataxia, has occasionally been observed within one individual or family (Jankovic and Demirkiran, 2001).

Molecular genetic analyses of multiplex families resulted in the identification of a few loci and lent further support to the hypothesis of a common genetic cause for paroxysmal dyskinesia/epilepsy/ataxia. Pure PKD was mapped to the peri-centromeric region of chromosome 16 (Kato *et al.*, 2006), but the causative gene is unknown (Kikuchi *et al.*, 2007); several families with infantile convulsions and PKD (Szepetowski *et al.*, 1997; Lee *et al.*, 1998; Swoboda *et al.*, 2000; Kato *et al.*, 2006) and a family with autosomal recessive rolandic epilepsy, PED and writer's cramp also map to the same chromosome 16 region (Guerrini *et al.*, 1999); pure PNKD maps to chromosome 2q33–q35, and the myofibrillogenesis regulator 1 (*MR-1*) gene was identified as causative (Rainier *et al.*, 2004). A family with paroxysmal dyskinesia/ataxia precipitated by exercise, emotional stress, sleep deprivation and alcohol consumption was mapped to chromosome 1p (Auburger *et al.*, 1996). A family with PNKD and generalized epilepsy mapped to chromosome 10q22, in which the α-subunit of a calcium-sensitive potassium channel (*KCNMA1*) is mutated (Du *et al.*, 2005). A third defective gene, the *MCT8* gene, is known to cause an X-linked form of PKD with severe global retardation (Brockmann *et al.*, 2005).

PED is a rare form of paroxysmal dyskinesia with approximately 20 sporadic patients and 9 PED families reported (Lance, 1977; Plant *et al.*, 1984; Nardocci *et al.*, 1989; Wali, 1992; Demirkiran and Jankovic, 1995; Auburger *et al.*, 1996; Bhatia *et al.*, 1997; Kluge *et al.*, 1998; Neville *et al.*, 1998; Guerrini *et al.*, 1999, 2002; Nagamitsu *et al.*, 1999; Margari *et al.*, 2000; Munchau *et al.*, 2000; Bing *et al.*, 2005; Kamm *et al.*, 2007). The co-occurrence of PED and epilepsy has been occasionally noted (Plant *et al.*, 1984; Bhatia *et al.*, 1997; Neville *et al.*, 1998; Guerrini *et al.*, 1999, 2002; Margari *et al.*, 2000; Munchau *et al.*, 2000; Bing *et al.*, 2005; Kamm *et al.*, 2007). Here, we describe the clinical, biochemical, imaging, electrophysiological and therapeutic aspects of a syndrome characterized by co-occurring PED and epilepsy. We elucidate its molecular pathophysiology consisting of a decreased transport of glucose across the blood-brain-barrier (BBB) due to mutations in the facilitative glucose transporter type 1 (GLUT1).

Material and Methods

Ascertainment and determination of phenotypes

We identified 56 members of a five-generation Belgian family (family A) with PED and epilepsy (Fig. 1). Thirty-nine family members participated in the genetic study. We interviewed and

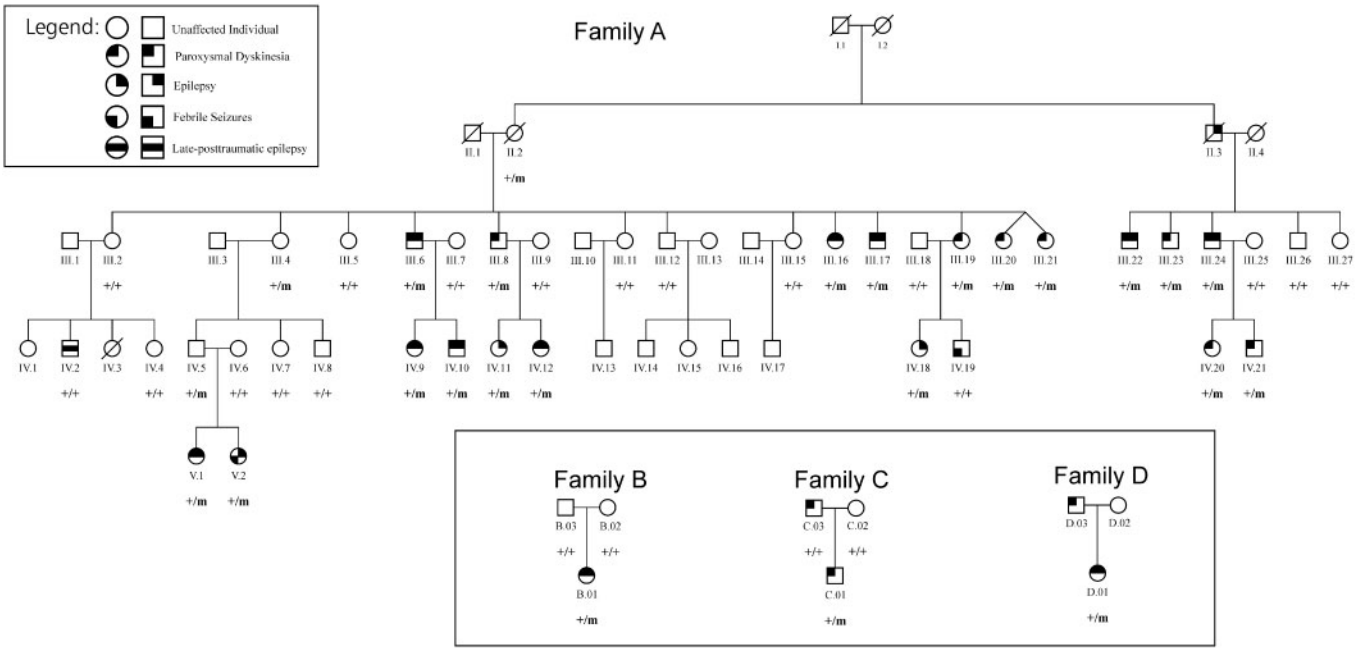

Fig. 1 Pedigree of families A–D. + = normal allele; m = mutated allele. Individuals carrying a heterozygous mutation in *SLC2A1* are indicated with +/m. Individuals indicated with +/+ do not carry a mutated allele. Individuals without indication were not available for screening.

performed a clinical neurological examination in 36 of them. For the other three individuals (II.2, III.4 and III.21), also carrying a mutation, we only obtained clinical information from their relatives and medical reports, when available. Three unrelated nuclear families of Belgian (families B and C) and Ashkenazi Jewish ancestry (family D), were subsequently evaluated. Available interictal and ictal EEGs, and video-EEG recordings were reviewed. Patients were diagnosed with epilepsy when experiencing recurrent generalized tonic–clonic, absences, myoclonic (D.01) or complex partial seizures. We also reviewed available brain MRI scans, and performed 4- to 8-h-fasting serum glucose and cerebrospinal fluid (CSF) glucose concentration studies. We used the following scale to score frequency of PED and epileptic seizures: 5: daily, 4: weekly, 3: monthly, 2: yearly, 1: remission >1 year, 0: no history of epilepsy or PED. The ethical committees of University Hospital Gasthuisberg and University of Antwerp approved this study and a written informed consent was obtained from all participants or their legal representative.

Linkage analysis

Thirty-nine family members from family A were genotyped using an in-house genome-wide mapping panel containing 425 autosomal microsatellite markers with an average marker distance of 7.8 cM and a maximum marker distance of 15.3 cM. Genetic analyses were performed as described elsewhere (Deprez *et al.*, 2007). Additional markers in the candidate region between D1S233 and D1S405 were selected from the Marshfield comprehensive genetic map (http://research.marshfieldclinic.org/genetics/) and the ABI Prism Linkage Mapping Set MD-10 and MD-5 (Applied Biosystems, Foster City, CA, USA) for the fine mapping of the region.

Two-point logarithms of odds (LOD) scores were calculated using MLINK from the FASTLINK computer package (version 5.1) (Cottingham *et al.*, 1993). The affected status of individuals was defined before linkage analysis. All patients with PED and/or epilepsy were considered affected. LOD-scores were calculated under the assumption of a dominant inheritance pattern with 95% penetrance and a disease gene frequency of 0.001. The estimation of the penetrance of the epileptic trait was based on the pedigree of the entire family. For each marker, the number of alleles was set at the observed number of alleles in the pedigree and we assumed these alleles to be equifrequent.

Mutation analysis

Mutation analysis of all exons and intron–exon boundaries of *SLC2A1* was performed on genomic DNA of eight family members of family A and all available members of families B–D by PCR sequencing. Purified PCR products were subsequently sequenced using the ABI BigDye Terminator cycle sequencing kit v3.1 and analysed on an ABI 3730 automated sequencer (PE Applied Biosystems, Foster City, CA, www.appliedbiosystems.com). Automated variation (SNPs and indels) discovery was performed using novoSNP (Weckx *et al.*, 2005). Subsequently, we used pyrosequencing (Alderborn *et al.*, 2000) to confirm the presence of the mutation in all patients and to exclude it in non-affected family members and a panel of 184 ethnically matched control individuals.

Functional analysis

The cDNA of *SLC2A1* in the expression vector pSP65 was kindly provided by Dr Mike Mueckler (Mueckler *et al.*, 1985). The QuickChange site-directed mutagenesis kit (Stratagene, LaJolla, Canada) was used to introduce the three missense mutations into the *SLC2A1* cDNA, resulting in p.S95I, p.V140M, p.N317T amino acid exchanges, respectively. Primer sequences are available upon request. All mutations were verified by direct sequencing.

All further procedures about the expression and functional characterization of the mutations compared with wild-type (WT) transporters in *Xenopus* oocytes, including the preparation of cRNA and oocytes, glucose uptake measurements in form of zero-trans influx experiments with 3-O-methyl-D-glucose, kinetic analysis to obtain K_m and V_{max}, Western blots and immunocytochemistry to study protein stability and surface expression, as well as Rb^+ flux experiments are described in detail elsewhere (Weber *et al.*, 2008). For the glucose uptake and Rb^+ flux studies, three experiments using 10 oocytes each for every glucose concentration (eight for Rb^+) were averaged for both mutant and WT transporters on each experimental day. The procedures for all four clones were done in parallel.

Functional imaging studies

Subjects

Fourteen patients with PED and epilepsy [8 F, 6 M; median age: 25 years (range: 13–52)] carrying a GLUT1 mutation were investigated using 2-[^{18}F]Fluoro-2-deoxy-D-glucose (FDG) PET. The metabolic results for the patient group were compared with FDG PET data from 20 age- and sex-matched healthy volunteers (11 F, 9 M; age range 21–49 years) that were obtained using the same acquisition protocol and scanner. The healthy volunteers had no history of neurological or psychiatric disorders and had normal findings on T_1- and T_2-weighted brain MRI. The patients had CSF and serum glucose studies immediately after the FDG PET scan, but not the control subjects.

PET

PET metabolic data acquisition was performed according to the standard clinical protocol (Van Laere *et al.*, 2006). FDG data were spatially normalized to Montreal Neurological Institute (MNI) space using statistical parametric mapping (SPM) (version 2; Wellcome Department of Imaging Neuroscience) with the standard settings. Normalized data were smoothed with an isotropic Gaussian kernel of 10 mm. A voxel-based group comparison of patient group versus controls was performed after proportional scaling the images (to compare the relative FDG uptake) and an initial statistical threshold $p_{uncorrected} < 0.001$ for peak height was used. Only clusters with a corrected $p_{cluster} < 0.05$ were considered significant. Furthermore, voxel-based correlations were evaluated between relative FDG uptake and CSF glucose, CSF/blood glucose ratio and age in the patient group and epileptic seizure frequency score and PED frequency score at time of FDG PET scanning in the patient and control group combined.

One patient had an ictal SPECT scan during a PED episode. We described the methodology of ictal SPECT previously (Dupont *et al.*, 2006).

Results

Genetics

Genome-wide linkage analysis of family A, showed several neighbouring markers on chromosome 1p35–p31 with LOD scores above 3.3 with a maximum of 5.72 for marker D1S2797 (Table: LOD scores; in Supplementary data). No other markers yielded LOD scores above 1.8. Segregation analysis identified a disease haplotype spanning a 19.7 cM region between markers D1S233 and D1S2652, comprising about 377 known genes, including *SLC2A1* encoding the GLUT1 glucose transporter. PCR sequencing of *SLC2A1* revealed a heterozygous missense mutation, p.S95I, in exon 4 due to a T-to-A and a C-to-T transition at two neighbouring nucleotides c.[283T>A;284C>T] (numbering according to cDNA reference sequence NM_006516.1, numbering started at A of the translation initiation codon, ATG). This mutation was identified in 22 of the 39 family members, co-segregated with the disease phenotype (Fig. 1) and was not present in 184 unrelated ethnically matched control individuals. We subsequently identified different mutations in *SLC2A1* in three non-related nuclear families with comparable phenotypes: a frameshift mutation (c.654dupC; p.N219QfsX18) in patient B.01 and missense mutations in patient C.01 (c.418G>A; p.V140M) and patient D.01 (c.950A>C; p.N317T). The mutations in B.01 and C.01 were not observed in their parents nor in healthy control individuals.

The four mutations (p.S95I, p.V140M, p.N219QfsX18 and p.N317T) were localized in the cytosolic loop connecting transmembrane segments 2 and 3, in transmembrane segment 4, in the large cytosolic loop connecting transmembrane segments 6 and 7 and in transmembrane segment 8, respectively (Fig. 2). The frameshift mutation (c.654dupC) predicts a premature stop codon at position 236 in the protein sequence, resulting in a truncated protein. Alignment of homologue protein sequences of different species with ClustalW (http://www.ebi.ac.uk/clustalw/) showed that the serine (position 95), valine (position 140) and asparagine (position 317) residues are highly conserved (alignments, see Supplementary data), supporting that these mutations are most likely pathogenic.

Clinical data

Of the 25 individuals (22 of family A, B.01, C.01 and D.01) carrying a mutation in *SLC2A1*, 19 had a history of PED (76%) and 14 of epilepsy (56%); 11 (44%) had a history of both. Three mutation carriers of family A (II.2, III.4 and IV.5) were asymptomatic, demonstrating reduced penetrance. Two individuals (IV.2; IV.19) who did not carry the mutation had late-posttraumatic epilepsy and febrile

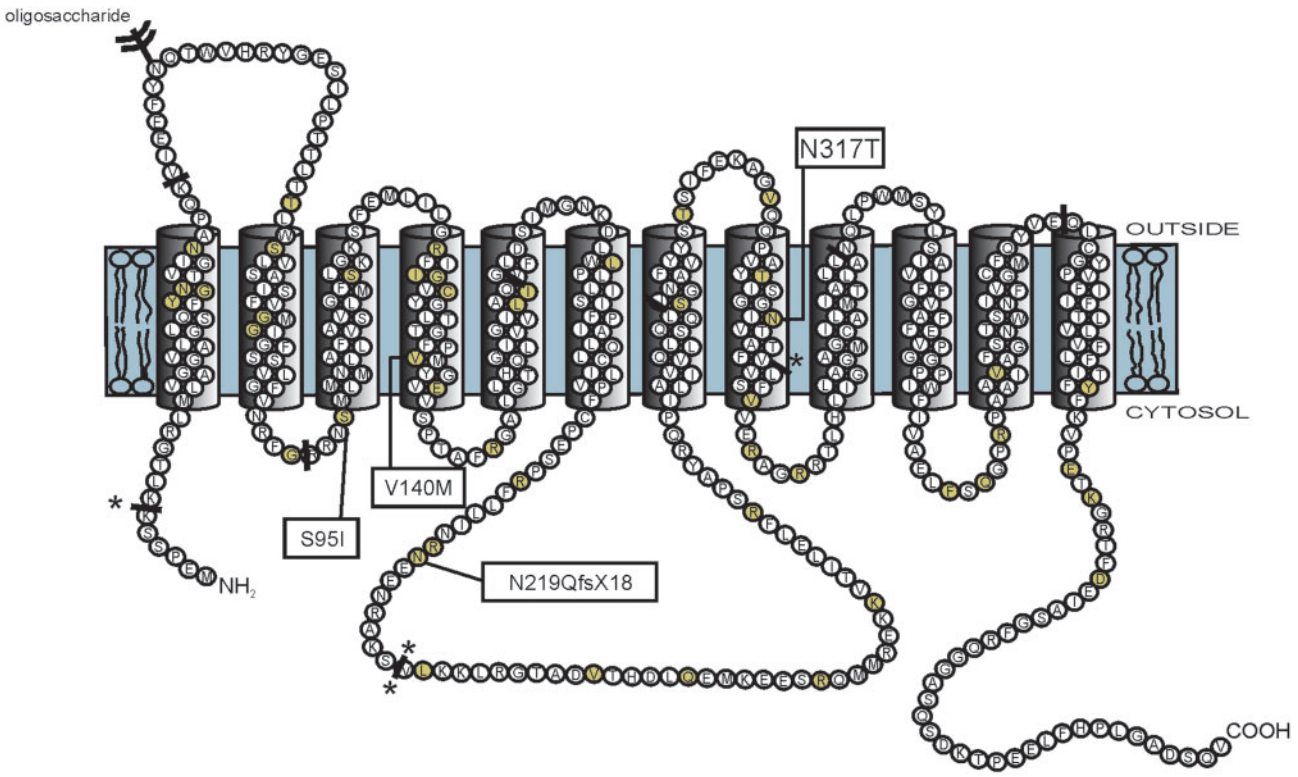

Fig. 2 The GLUTI protein structure consisting of I2 transmembrane domains and intracellular amino- and carboxy-termini (Mueckler *et al.*, I985). GLUTI DS (Klepper and Leiendecker, 2007) and PED/epilepsy mutations are marked on this figure (yellow colored circles). The PED/epilepsy mutations are boxed. The solid bars indicate the locations of the intron–exon boundaries in the *GLUTI* gene. Splice site mutations are indicated at these solid bars with asterisk.

seizures, respectively. The asymptomatic parents of B.01 did not carry the mutation, suggesting that the mutation in their child arose *de novo* (paternity was confirmed with the analysis of a panel of 31 STR markers located on 15 different chromosomes). Finally, in patient C.03, no mutation was observed. The son of C.03 (paternity was checked), C.01, had a similar clinical phenotype as his father (PED without epilepsy) and did carry a mutation in *SLC2A1*.

PED

Nineteen patients with an *SLC2A1* mutation had a history of PED (Tables 1 and 2). Median age at onset was 8 years (range: 3–30). In all studied patients involvement of the legs was present (100%), involving exclusively the legs in 10 (55%), legs more than arms in 6 (33%) and also the face in two of these 6 (11%). One patient reported that arms and legs were equally affected, and one that arms were affected more frequently than legs. The latter patient worked as a cleaner and reported PED involving the arms precipitated by exertion of the arms during cleaning. Nine patients (50%) reported a consistent lateralization, e.g. patient A.III.6 reported onset of the movement disorder always in the left leg. Nine patients (50%) reported involuntary movements suggestive of choreoathetosis alone, three (17%) of dystonia and six of both (33%). The patients described the choreoathetosis as uncontrollable rapid movements, and the dystonia as stiffening and cramps. PED made walking impossible, and caused falls in some of the patients. Some patients were able to stand despite the PED, or walk with difficulty, but most patients had to sit down until the movements subsided. Median duration of the PED was 15 min (range: <1 min to 3 h). Precipitating factors were exertion ($n = 16$, 89%), particularly prolonged brisk walking, stress ($n = 7$, 39%), starvation ($n = 5$, 28%) and sleep deprivation ($n = 1$, 6%). Alleviating factors were eating, preferably glucose or sugar ($n = 6$, 33%), and rest ($n = 7$, 39%). Patient A.III.19 remained symptom-free for several years by avoiding long walks. Patient A.III.8 remained symptom-free for

Table 1 Clinical data, EEG, MRI of the brain, serum and CSF glucose concentration

Id	G	Age (yr)	E	PED	EEG	MRI	PET	SG (mg/dl)	CSF G (mg/dl)	Ratio CSF G/SG (NI > 0.60)	AED ever used
A.II.2	F	70	/	/	/	/		/	/	/	/
A.III.4	F	57	/	/	/	/		/	/	/	/
A.III.6	M	53	+	+	NI	NI	Y	86	47	0.55	PB, PHT, LTG, LEV, CLB
A.III.8	M	50	–	+	NI	NI	Y	80	43	0.54	VPA
A.III.16	F	46	+	+	GS	NI	Y	83	41	0.49	VPA, TPM
A.III.17	M	43	+	+	GSW, GS, PS	NI	Y	87	50	0.57	VPA, LEV, CBZ, PHT
A.III.19	F	42	–	+	/	/	Y	105	49	0.47	N
A.III.20	F	34	–	+	GSW	NI		/	/	/	VPA
A.III.21	F	34	U	+	S LFr	/		/	/	/	VPA
A.III.22	M	47	+	+	/	/		/	/	/	VPA, PHT
A.III.23	M	46	–	+	NI	/		/	/	/	CBZ, LTG, PHT
A.III.24	M	44	+	+	GSp, NI BG	NI	Y	86	41	0.48	VPA, PHT, LEV
A.IV.5	M	30	–	–	NI	/		/	/	/	N
A.IV.9	F	30	+	+	GSW, GSp, NI BG	NI	Y	85	41	0.48	VPA, CBZ, TPM
A.IV.10	M	30	+	+	GSW, PS, NI BG	NI		/	/	/	VPA, CBZ, PHT
A.IV.11	F	20	+	–	GSW, Sp, PS, NI BG	NI	Y	65	34	0.52	VPA, ESM, LTG, CLB
A.IV.12	F	15	+	+	GSW, NI BG	NI	Y	78	38	0.49	VPA, LTG
A.IV.18	F	16	+	–	NI	NI	Y	76	41	0.54	VPA
A.IV.20	F	13	–	+	NI	NI	Y	75	40	0.53	VPA
A.IV.21	M	14	–	+	S L	/	Y	81	48	0.59	VPA
A.V.1	F	7	+	+	3 Hz GSW, TA during HV, NI BG	NI		/	/	/	CBZ, VPA, LTG
A.V.2	F	5	+	–	NI	/		/	/	/	N
B.01[a]	F	23	+	+	S LT	NI	Y	83	41	0.49	VPA, LTG
C.01	M	22	–	+	NI	NI	Y	94	45	0.48	VPA, GBP
C.03	M	47	–	+	/	/		107	64	0.60	/
D.01	F	22	+	+	NI	/		/	/	/	N
							Range	65–107	34–64	0.47–0.60	
							Mean ± SD	85 ± 11	44 ± 7	0.52 ± 0.04	

[a]Only patient with abnormal neuronal examination (Mild ataxia, dysarthria, deep tendon reflexes L > R, Babinski sign L).
Id = identification; G = gender; F = female; M = male; yr = years; / = information not available; NI = normal; L = left; R = right; E = epilepsy; U = unknown; + = yes; – = no; EEG = electroencephalogram; GSW = generalized spike wave; GS = generalized slowing; PS = polyspikes; GSp = generalized spikes; S = slowing; Sp = spikes; Fr = frontal; T = temporal; BG = background; TA = typical absence; HV = hyperventilation; MRI = magnetic resonance imaging; PET = positron emission tomography; SG = serum glucose concentration; CSF G = cerebrospinal fluid glucose concentration; AED = antiepileptic drug; VPA = valproate; PB = phenobarbital; PHT = phenytoin; LTG = lamotrigine; LEV = levetiracetam; CLB = clobazam; TPM = topiramate; CBZ = carbamazepine; GBP = gabapentin; ESM = ethosuximide.

Table 2 Paroxysmal exercise-induced dyskinesia

Id	Age at onset (yr)	Localization	Lateralization	Clinical manifestations	Duration (min)	Precipitating factors	Alleviating factors	Worst frequency during lifetime	PED frequency score
A.III.6	7	Le > A > Fa	L > R	CA	3–45	Ex, S, STA	E, Re	3	3
A.III.8	8	Le > A	L > R	CA	2–15	Ex	E, Re	3	1
A.III.16	± 20	Le	R = L	CA	5	S	U	4	1
A.III.17	30	Le	R = L	CA	<1	Ex	U	4	4
A.III.19	10	Le	R = L	D	5	Ex	E, Re	3	1
A.III.20	8	A > Le	R > L	CA, D	U	Ex	U	U	U
A.III.21	U	U	U	U	U	U	U	U	U
A.III.22	10	Le	R > L	CA	3	Ex	U	3	2
A.III.23	9	Le	L > R	CA	30–45	Ex, S	U	5	2
A.III.24	8	Le > A > Fa	L > R	CA, D	15–30	Ex, S, STA	E, Re	4	4
A.IV.9	7	Le > A	R > L	CA, D	60	Ex, S, STA	E	5	4
A.IV.10	3	Le > A	R > L	CA	2–180	Ex, STA	U	3	1
A.IV.12	6	Le	R > L	CA, D	2–5	Ex	U	5	5
A.IV.20	3	Le	R = L	CA	30–60	Ex	U	2	2
A.IV.21	13	Le	R = L	D	30	Ex	U	2	2
A.V.1	6	A = Le	R = L	CA	U	S	U	2	2
B.01	5	Le	R = L	CA, D	15–30	Ex	Re	5	2
C.01	7	Le	R = L	CA, D	5–30	Ex, S	E, Re	4	4
C.03	± 20	Le	R = L	CA, D	5–10	Ex	R	4	4
D.01	10	Le > A	R = L	D	1–5	Ex, STA, sleep deprivation	Re	4	4

Id = identification; yr = years; Le = legs; A = arm; Fa = face; U = unknown; L = left; R = right; CA = choreoathetosis; D = dystonia; STA = starvation; Ex = exertion; S = stress; E = eating; Re = rest; PED frequency score: 5 = daily; 4 = weekly; 3 = monthly; 2 = yearly; 1 = remission > 1 year.

several decades by changing his diet and having a sugar-containing snack every 2–3 h. C.01 always carried a bottle of sugar-containing beverage, which reduced the PED episodes. The PED at its worst occurred on average weekly (ranging between patients from several attacks daily to yearly) and at the latest assessment on average yearly (ranging between patients from weekly to remission of symptoms). Most patients reported that PED and epilepsy became less severe when they grew older. Some patients reported autonomic symptoms, such as sweating, pallor, hyperventilation, a rising epigastric sensation, psychic symptoms, such as anxiety and sensory symptoms, such as paraesthesiae, a few minutes before the onset of the dyskinesias. The treating neurologists often interpreted the PED as epileptic myoclonic jerks as part of juvenile myoclonic epilepsy.

Epilepsy

Fourteen mutation carriers had epilepsy (Tables 1 and 3). Median age at onset was 2 years (range: 0–19). Seizure types were absences ($n = 9$, 64%), generalized tonic–clonic seizures without focal onset ($n = 7$, 50%), complex and simple partial seizures ($n = 2$, 14%), febrile seizures ($n = 1$, 7%), myoclonic seizures and myoclonic status epilepticus ($n = 1$, 7%). One patient with partial seizures (A.IV.11) reported unformed visual hallucinations, a rising epigastric

Table 3 Epilepsy

Id	Age at onset (yr)	Seizure types	Worst seizure frequency during lifetime	Seizure frequency at assessment
A.III.6	3	A, GTCS	3	1
A.III.16	0	GTCS	2	1
A.III.17	19	GTCS	3	3
A.III.22	8	A, GTCS	3	3
A.III.24	8	A	4	3
A.IV.09	0	A	5	1
A.IV.10	0	GTCS	2	1
A.IV.11	5	CPS, A, SPS	5	4
A.IV.12	2	CPS, GTCS, SPS	2	1
A.IV.18	2	GTCS	2	1
A.V.1	2	CSE, TA	5	1
A.V.2	1	A, FS	2	1
B.01	2	A	4	1
D.01	19	M, MSE	5	4

Id = identification; yr = years; A = absence; GTCS = generalized tonic–clonic seizure; CPS = complex partial seizure; SPS = simple partial seizure; TA = typical absence; CSE = convulsive status epilepticus; FS = febrile seizure; M = myoclonus; MSE = myoclonic status epilepticus; seizure frequency: 5 = daily; 4 = weekly; 3 = monthly; 2 = yearly; 1 = remission > 1 year.

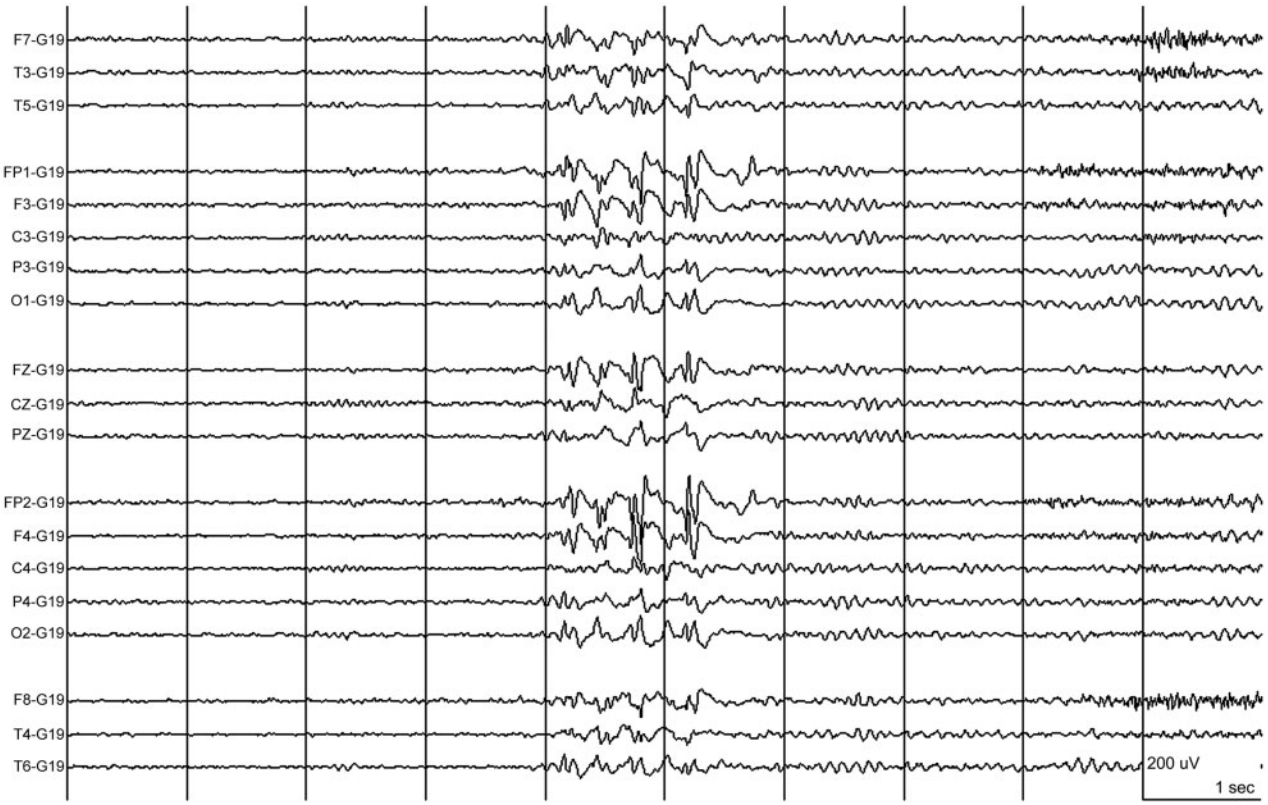

Fig. 3 The interictal EEG of patient A. III.24 showed high voltage anterior predominant generalized spike-wave complexes on a normal background. Time base: 30 mm/s, sensitivity: see calibration: 200 μV/cm, high cut: 30.0 Hz, low cut: 0.5 Hz.

sensation and nausea followed by loss of awareness, staring and dystonic posturing of the right arm lasting around one minute. The other patient with partial seizures (A.IV.12) had simple partial seizures characterized by visual and auditory hallucinations followed by secondary generalized tonic–clonic seizures and postictal confusion. For most of the patients seizure remission was easily obtained with antiepileptic drug treatment.

Other paroxysmal phenomena

One patient (A.IV.21) had as first manifestation of the disease an episode of aphasia and right hemiparesis lasting around 60 min at the age of 13 years. One patient (A.III.17) had an episode of quadriparesis with preserved consciousness lasting around 30 min. C.01 frequently had aggressive outbursts, requiring psychiatric treatment.

Mental status

Most mutation carriers were of average intelligence or had mild mental retardation. Four patients (A.III.16, A.IV.10, A.IV.11 and A.IV.12) underwent formal neuropsychological testing and had a median IQ of 65 (range: 45–79). The patient with an IQ of 45 (A.III.16) was the only family member living in a sheltered home. No difference was observed between the intelligence level of epilepsy patients and pure PED patients.

EEG

EEG studies were performed in 21 mutation carriers of families A–D. The EEGs were normal ($n = 9$, 43%), showed interictal generalized epileptic discharges on a normal background ($n = 6$, 29%) (Fig. 3), interictal generalized epileptic discharges with mild to moderate background slowing ($n = 2$, 10%), generalized mild background slowing ($n = 1$, 5%) and focal slowing ($n = 3$, 14%). Epileptic discharges were predominant over anterior brain regions. One child (A.V.1) had two witnessed typical absences during hyperventilation with 3 Hz generalized spike-wave discharges on EEG with a normal background (Fig. 4, Table 1). Seven patients underwent video-EEG monitoring, including the proband of family A (IV.12) as well as patients A.III.17, A.III.20, A.III.24, A.IV.11, B.01 and C.01). During the video-EEG recordings, patient A.III.24 had two episodes of paroxysmal choreoathetosis lasting around 10 and 20 min each, and involving mainly both legs. The movements were characterized by sudden kicking and bending movements of the legs, with twisting and trusting movements of the pelvis (see video; A.III.24 Ictal SPECT during PED, in supplementary data). Ictal EEGs did not show epileptic activity. We recorded a nocturnal generalized tonic–clonic seizure on video-EEG in patient A.III.17, which started with a 1 s burst of polyspikes on EEG, followed by generalized slow sharp waves admixed with spikes, which became gradually obscured by muscle artefacts. In the proband

Fig. 4 During hyperventilation, patient A.V.I had a brief absence with high voltage 3 Hz generalized spike wave discharges during 6 s on EEG. Time base: 30 mm/s, sensitivity (of original recording): 300 μV/cm, high cut: 35.0 Hz, low cut: 0.5 Hz.

A.IV.12, we recorded some mild episodes of gait difficulties during prolonged walking, during which she complained of pain and shakiness in the left leg, without objective signs and no ictal EEG changes. We recorded one of the episodes of B.01 during video-EEG recording, which was precipitated by prolonged walking. Her gait became slightly broad based, she stumbled and her legs appeared to stiffen. She was unable to walk unassisted. She recovered within 10 min. C.01 underwent several prolonged video-EEG recordings that did not show epileptic activity.

Neurological examination

Neurological examination was normal in all mutation carriers, except B.01. Her speech was dysarthric, there was mild appendicular ataxia and deep tendon reflexes on the left were brisker than on the right, with Babinski sign on the left.

Serum and CSF glucose studies

After identifying the mutations in GLUT1, 14 mutation carriers underwent a 4- to 8-h-fasting serum glucose and CSF glucose concentration study. The median ratio of CSF glucose/serum glucose concentration was 0.52 (range in our patients: 0.46–0.59, normal: >0.60). Median CSF lactate was 1.23 mmol/l (range: 0.87–1.36, normal: 0.60–2.20). Median CSF protein concentration was 376 mg/l (range: 264–664, normal: 150–450). Also, the one patient without a demonstrable *SLC2A1* mutation (C.03) had a lower than normal ratio of CSF glucose/serum glucose concentration.

Functional studies

We introduced all three missense mutations into the cDNA of GLUT1 and expressed WT and mutant (S95I, V140M, N317T) transporters in *Xenopus* oocytes. Glucose uptake was largely reduced for all mutations compared with WT transporters (Fig. 5A). A kinetic analysis of the uptake experiments in oocytes revealed that all mutations lead to a decrease of the maximum transport velocity, V_{max}, by at least 3- to >10-fold, while we observed no marked change and definitely no increase of the Michaelis-Menten constant, K_m, for mutant compared with WT transporters (Fig. 5B and Figure legend). Western blots suggested an equal production and stability of the mutant proteins compared with the WT (Fig. 5C). Immunocytochemistry indicated that all three mutants were properly inserted in the cell surface membrane, similar to the WT (Fig. 5D).

As an ionic leak for another GLUT1 mutation inducing increased $^{86}Rb^{+}$ flux was observed by some of us in a family in which PED is combined with haemolytic anaemia (Weber *et al.*, 2008), we also performed $^{86}Rb^{+}$ flux experiments with all three mutations. As expected, we did not observe a significant difference in $^{86}Rb^{+}$ flux compared with the WT and water-injected oocytes, indicating that these mutations do not induce an ionic leak of the GLUT1 transporter. This corresponds well to the fact that the respective patients did not show signs of haemolytic anaemia.

Imaging

FDG PET: group-based comparison

The group comparison of patients with co-occurring PED and epilepsy and controls resulted in a relatively increased glucose metabolism in the putamen (x, y, $z = -28$, 4, 10;

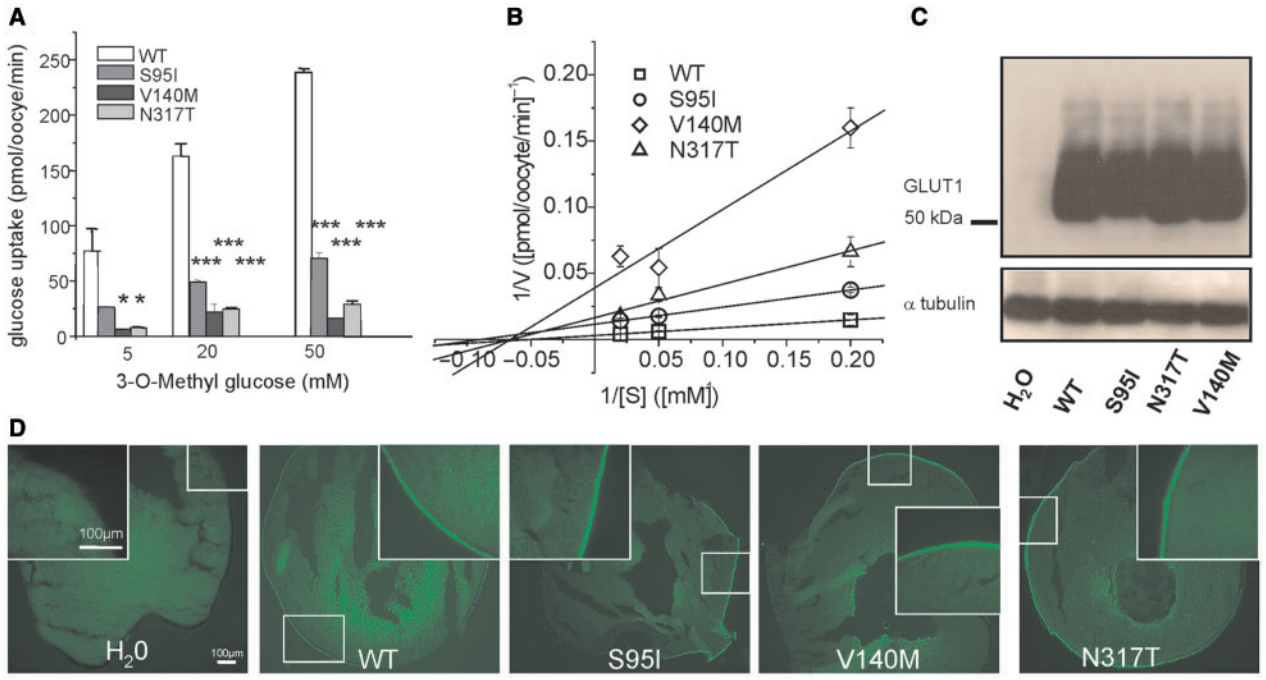

Fig. 5 Functional studies to investigate a change in glucose uptake, protein stability or trafficking by the three point mutations in *Xenopus* oocytes. (**A**) Plotted is the glucose uptake versus 3-O-methyl-D-glucose (OMG) concentration. The uptake was significantly reduced for all three mutations (shown are representative results recorded from one batch of 3×10 oocytes for each glucose concentration, means ± SEM, $^{*}P < 0.05$, $^{***}P < 0.001$). (**B**) Kinetic analysis of glucose uptakes in oocytes according to Lineweaver-Burk. The linear function $1/V$ ($1/[S]$) = $1/V_{max} + K_m/V_{max}{}^{*}1/[S]$ was fit to the data points, with [S] being the concentration of OMG, V the uptake velocity in pmol/oocyte/min obtained for a given [S], V_{max} the maximal uptake velocity reflecting the maximal transport capacity of GLUT1 and K_m the Michaelis-Menten constant representing the concentration [S] for which the half-maximal uptake velocity ($V_{1/2}$) is reached. V_{max} and K_m were calculated from the *y*- and *x*-interceptions of the linear fits, with the *y*-intercept equalling $1/V_{max}$ and the *x*-intercept $-1/K_m$. The following values were obtained (V_{max} is given in pmol/oocyte/min and K_m in mM): WT: $V_{max} = 319 \pm 16$, $K_m = 19 \pm 1$; S95I: $V_{max} = 86 \pm 2$, $K_m = 11 \pm 1$; V140M: $V_{max} = 26 \pm 11$, $K_m = 15 \pm 9$; N317T: $V_{max} = 60 \pm 18$, $K_m = 15 \pm 7$. (**C**) Western blots obtained from oocytes injected with equal amounts of cRNA showed a similar amount of protein for all mutations and the WT, but no respective band for oocytes injected with H_2O as a negative control; α-tubulin was used as a loading control. (**D**) Immunocytochemical analysis of injected oocytes using an anti-GLUT1 antibody revealed similar stainings of the surface membranes for all four clones.

$p_{cluster} < 0.001$; *x*, *y*, *z* = 32, −6, 10; $p_{cluster} = 0.003$) and midtemporal cortex bilaterally (*x*, *y*, *z* = −54, −34, 2; $p_{cluster} = 0.031$; *x*, *y*, *z* = 48, −36, 4; $p_{cluster} = 0.011$). There was also relative hypermetabolism in the right lingual cortex (*x*, *y*, *z* = 24, −82, −2; $p_{cluster} = 0.004$). Glucose metabolism was relatively decreased in patients compared with controls bilaterally in thalamus (*x*, *y*, *z* = 18, −20, 16; $p_{cluster} < 0.001$; *x*, *y*, *z* = −14, −24, 14; $p_{cluster} < 0.001$), anterior cingulate cortex (*x*, *y*, *z* = 8, 2, 42; $p_{cluster} < 0.001$), midfrontal and superior frontal cortex (*x*, *y*, *z* = 18, −2, 52; $p_{cluster} < 0.001$; *x*, *y*, *z* = −8, 52, 40; $p_{cluster} < 0.001$) (Fig. 6).

Correlation analysis

No significant correlation between relative FDG uptake and CSF glucose or CSF/blood glucose ratio was found. There was also no correlation with age. However, we found a negative correlation between relative FDG uptake and the epileptic seizure frequency score at the time of PET scanning in the midfrontal and cingulate cortex bilaterally (*x*, *y*, *z* = −28, 20, 56; $p_{cluster} < 0.001$; $r = -0.72$). When a patient suffered from more frequent seizures, the hypometabolism was more pronounced in this brain region.

There was a positive correlation between relative FDG uptake and the PED frequency score at time of PET scanning in the left putamen (*x*, *y*, *z* = −32, 6, 6; $p_{cluster} = 0.013$; $r = 0.67$) and a negative correlation in the left superior frontal cortex (*x*, *y*, *z* = −16, 30, 50; $p_{cluster} = 0.001$; $r = -0.71$) and left anterior cingulate cortex (*x*, *y*, *z* = −4, 30, 20; $p_{cluster} = 0.006$; $r = -0.59$) extending to the right side (*x*, *y*, *z* = 8, 40, 18). When a patient suffered from more frequent PEDs, the frontal lobe hypometabolism was more pronounced, as was the relative hypermetabolism in the putamen.

Ictal SPECT

Ictal SPECT and interictal FDG PET of patient A.III.24 are shown in Fig. 7. Ictal SPECT showed hyperperfusion in left putamen and leg motor areas. These regions showed relative hypermetabolism and hypometabolism, respectively, on interictal FDG PET. The injected episode of PED started with dyskinesia in the left leg, but around 30 s after tracer

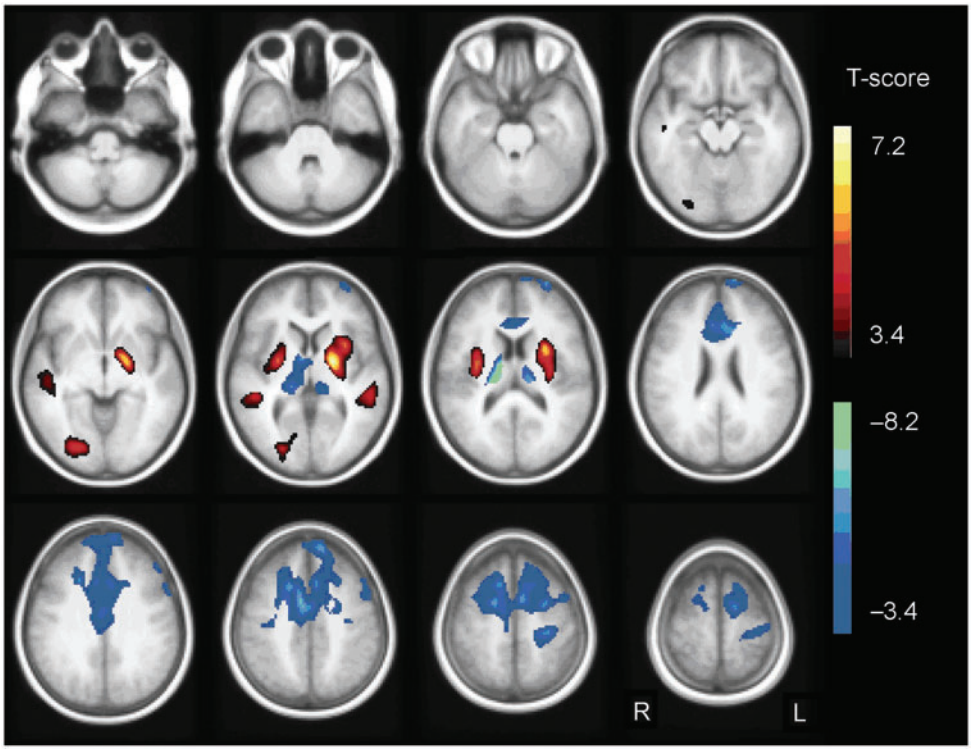

Fig. 6 SPM T-map of the analysis of patients versus controls. Relative hypermetabolism in the patient group compared with controls is indicated in yellow/red, hypometabolism in blue/green. Results are projected on an average spatially normalized in-house T1 image of healthy controls. R = right; L = left.

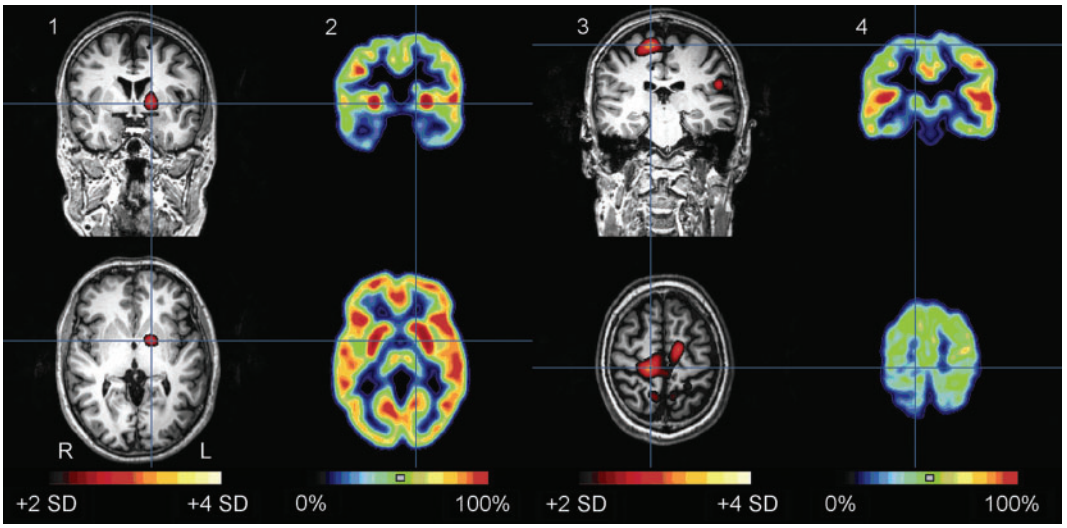

Fig. 7 Subtraction ictal SPECT coregistered to MRI (SISCOM) (1, 3) during an episode of PED and interictal FDG PET (2, 4) in patient A.III.24. Top row: coronal images, bottom row: axial images. The episode of PED lasted in total around 17 min, and was interrupted by brief moments of no abnormal movements. The dyskinesia mainly involved the legs, left more than right and pelvis (see video; A.III.24 Ictal SPECT during PED, in supplementary data). The injection was given around three minutes after onset. The SISCOM (threshold: + 2 SD) showed an area of hyperperfusion in the left putamen (blue cross in 1), which coincided with interictal putaminal hypermetabolism (blue cross in 2). The largest and most hyperintense hyperperfusion cluster was in the right primary motor area of the leg (blue cross in 3), which coincided with an area of hypometabolism in the interictal FDG PET (blue cross in 4). All images are coregistered. Hyperperfusion clusters are projected on the patient's MPRAGE images. R = right; L = left.

injection, the abnormal movement involved both legs, right more than left (see video; A.III.24 Ictal SPECT during PED, in supplementary data).

Therapy

Carbohydrate-rich diet

Because sugar and food intake was reported as an alleviating factor in our families, we started patients A.III.17, A.III.24, A.IV.11 and A.IV.12 on a carbohydrate-rich diet, with additional frequent carbohydrate-containing snacks at regular intervals (every 3–4 h). There was no improvement, and patient A.III.24 reported that frequency and intensity of PED attacks had worsened.

Ketogenic diet

Since a ketogenic diet is reportedly effective in GLUT1 DS (De Vivo *et al.*, 1991; Leary *et al.*, 2003; Klepper *et al.*, 2004), this was initiated in patients A.III.17, A.IV.11 and A.IV.12. The diet consisted of a strict 3 : 1 proportion of fat [3] to protein and carbohydrates [1], fat being supplied in the form of medium-chain triglyceride mix (Liquigen®, from SHS Nutricia, Liverpool, UK; http://www.shs-nutrition.com/shs-product/liquigen). In addition, all patients received L-carnitine (50 mg/kg) and all necessary vitamin and trace element supplements. The establishment and follow-up of ketosis was checked twice daily with urine dip sticks. Patient A.IV.12, who demonstrated 4–5 episodes daily of PED (cramping of the left leg, inability to walk >50–100 m without pausing or dystonia) before starting on the diet, showed immediate (same day) response when reaching ketosis. She had complete resolution of PED and was able to walk and even run long distances for the first time in her life. As soon as ketosis was lost, e.g. due to diet non-compliance, symptoms recurred. Patients A.III.17 and A.IV.11 have been free of epileptic seizures, since the start of the ketogenic diet (now 2 months—previous frequency of seizures once weekly in patient A.IV.11 and once monthly in patient A.III.17). None of the other 21 mutation carriers of family A were willing to start a ketogenic diet, because in their opinion the advantages did not outweigh the disadvantages of the disease and diet itself.

Discussion

Genetics and molecular pathophysiology of PED and epilepsy

Our study indicates that both PED without epilepsy and co-occurrence of PED with epilepsy can be caused by mutations in *SLC2A1*, which encodes GLUT1, the main transporter for D-glucose across the BBB. To date, we have screened four PED families with or without epilepsy and detected novel *SLC2A1*/*GLUT1* mutations (three missense and one frameshift) in all of them. In a parallel investigation, Weber and colleagues screened another five PED families and identified GLUT1 mutations in three of them (Weber *et al.*, 2008). Both studies suggest that mutations in GLUT1 may be the most common cause in this condition. While our identified frameshift mutation predicts a complete loss of function and haploinsufficiency, the functional investigations in oocytes showed that all three missense mutations also lead to a marked reduction of glucose uptake. The mutations affect the intrinsic ability of GLUT1 to transport glucose across the cell membrane by reducing the maximum transport velocity, V_{max}, whereas K_m, protein stability and insertion in the surface membrane did not show major alterations. Hence, attacks of PED can be caused by a reduced glucose transport across the BBB, possibly when the energy demand of the brain overcomes its supply after prolonged periods of exercise.

Clinical aspects, differentiation from classical GLUT1-DS and genotype–phenotype correlations

The characteristic clinical features in our patients were PED and epilepsy. PED consisted of choreoathetosis and dystonia affecting mainly the legs and was typically precipitated by prolonged exertion. Epileptic seizures in these patients appeared mainly as primary generalized, namely as generalized tonic–clonic or absences, with a much earlier onset than classical absence seizures. One patient had myoclonic seizures and two patients also had partial seizures. Interestingly, the choreoathetotic PEDs were often misdiagnosed as epileptic myoclonic seizures as part of juvenile myoclonic epilepsy. The young age at onset of the epilepsy around 2 years in combination with a family history of epilepsy and PED are important clinical clues to suggest the correct diagnosis of this treatable disease. We conclude that childhood-onset intractable exercise-induced dyskinesias, sometimes with co-occurring early-onset generalized epileptic seizures, normal neurological examination and MRI and a moderately low CSF glucose concentration are the key features of this recognizable clinical entity caused by GLUT1 mutations.

Heterozygous mutations in *SLC2A1* are also known to cause a rare, severe syndrome first described by De Vivo and colleagues in isolated patients, the GLUT1 DS (OMIM #606777) (De Vivo *et al.*, 1991; Klepper and Leiendecker, 2007). Most were demonstrated to be total loss-of-function mutations while other mutations caused a significant decrease in transport activity (Klepper *et al.*, 2001*a*; Iserovich *et al.*, 2002), as observed for our mutations. It is characterized by intractable infantile epileptic seizures, acquired microcephaly, hypotonia, ataxia, spasticity, developmental delay and a persistent reduced CSF/serum glucose concentration ratio. Exercise-induced dyskinesias, normal interictal neurological examination (except one, B.01), the absence of microcephaly, a different non-nutrition-dependent form of generalized epilepsy and the later age at onset differentiate our patients from patients with classical GLUT1 DS. Other important differences between our patients and the classical GLUT1 DS patients

were the less pronounced decrease in fasting CSF glucose to serum glucose concentration ratio (severe GLUT1 DS: median 0.33; PED and epilepsy: median 0.52 and normal: >0.60) and apparent improvement in symptomatology over time in our large family A. Most patients with classical GLUT1 DS tended to be so severely affected that they were not able to live independently, to marry and have children, and hence transmit the disease.

Some patients with an atypical clinical presentation and GLUT1 mutations were reported in the literature: three without infantile seizures, one with choreoathetosis and one with a prominent movement disorder (Overweg-Plandsoen *et al.*, 2003; Wang *et al.*, 2005; Friedman *et al.*, 2006). In the latter two patients, the movement disorder was characterized by childhood-onset paroxysmal episodes of blinking and abnormal head and eye movements without definite seizures in one patient and by intermittent facial and hand dystonia and mild choreatiform movements of the legs at rest in the other patient (Wang *et al.*, 2005; Friedman *et al.*, 2006). Also, three nuclear families with GLUT1 DS were reported to date, in which the phenotype between family members varied from intractable epileptic seizures with moderate mental retardation to controllable epileptic seizures with mild mental retardation (Brockmann *et al.*, 2001; Ho *et al.*, 2001; Klepper *et al.*, 2001*b*). These milder variants of GLUT1 DS, also proposed by Wang and colleagues (Wang *et al.*, 2005), have not been well documented, but in none of all GLUT1 DS patients described in the literature so far, the complex movement disorder has ever been described as exercise-induced dyskinesias with periods lasting from less than a minute to several hours. Also generalized forms of epilepsy as observed in our patients have not been described (Klepper and Leiendecker, 2007). These patients can thus be clearly differentiated from PED with epilepsy described here.

Although missense mutations in the cytosolic loop connecting transmembrane segments 2 and 3, in transmembrane segment 4 and in transmembrane segment 8 have been described in GLUT1 DS patients, the specific amino acid residues mutated in our patients have not been related to the pathophysiology of classical or atypical GLUT1 DS (Fig. 2). It appears that complete loss-of-function mutations rather cause classical GLUT1 DS, but other genetic or environmental factors have to play an important role in the expression of the clinical phenotype as well, since we also identified a loss-of-function mutation in one of our PED patients (B.01) and since we could not find an obvious difference in the uptake studies to the published point mutations causing classical GLUT1 DS (Brockmann *et al.*, 2001; Klepper *et al.*, 2001a, 2005; Wang *et al.*, 2003; Wong *et al.*, 2007). However, the S95I mutant yielded the mildest phenotype with cases of non-penetrance (A.II.2, A.III.4 and A.IV.5; who all passed the range of onset age for PED and epilepsy of this family) and also had the mildest deficit in glucose transport *in vitro*. As described for classical and atypical GLUT1 DS, no clear correlation was observed between the CSF glucose concentration and the type of mutation in our study.

Finally, in one patient (C.03) we did not observe an *SLC2A1* mutation despite his clinical phenotype and mildly reduced CSF/serum glucose ratio. However, this patient has an affected son (C.01) with an *SLC2A1* mutation that could be explained by a mosaicism.

Functional imaging and systemic pathophysiology of PED and epilepsy

Relative FDG uptake in our patients with PED and epilepsy was increased in the putamen, midtemporal cortex bilaterally and right lingual brain area, and decreased bilaterally in thalamus, anterior cingulate cortex, midfrontal and superior frontal cortex, when compared with a cohort of matched controls. These findings are principally comparable with the 'metabolic footprint of GLUT1DS on the brain' described by Pascual and colleagues (2002). However, a detailed comparison with this previous study, is difficult since Pascual and colleagues used visual analysis of individual PET scans and provided single PET sections of 14 patients without indication of scaling, whereas we performed a more objective voxel-based statistical analysis of grouped data in comparison to normal controls.

Our method allowed us to perform exploratory correlation studies enabling new hypotheses. We found a positive correlation between relative FDG uptake and the PED frequency score in the left putamen and a negative correlation in the left superior frontal cortex and bilateral anterior cingulate cortex. In addition, the ictal SPECT analysis revealed hyperperfusion in the same regions during an episode of PED. These findings suggest that disordered glucose metabolism in the corticostriate pathways plays a role in the pathophysiology of PED. Furthermore, we found a negative correlation between seizure frequency and relative glucose uptake in the midfrontal and cingulate cortex bilaterally. These observations implicate a disordered glucose metabolism in the frontal lobes in the pathophysiology of the epileptic seizures in our patients, which is consistent with our EEG findings of generalized epileptic discharges with anterior predominance. It should be pointed out that both Pascual's and our study used non-quantitative, radioactivity distribution and not quantitative, regional cerebral glucose utilization (rCMRglc) PET data. This method allowed us to study the pattern of relative FDG uptake (Signorini *et al.*, 1999), but not global cerebral changes, which may be present in persons with GLUT1 mutations. This is a shortcoming of the present study, which warrants further investigation.

Treatment

PED and epilepsy is associated with a low CSF glucose concentration in the presence of normoglycaemia. Although several family members reported that glucose and sugar alleviated symptoms, carbohydrate-rich diets have been

reported to be unsuccessful in classical GLUT1 DS (Wang *et al.*, 2005). A ketogenic diet (high fat, low carbohydrate) has been effective in patients with classical GLUT1 DS for management of intractable seizures and complex motor disorders, but had little effect on the cognitive impairment (De Vivo *et al.*, 1991; Leary *et al.*, 2003; Klepper *et al.*, 2004). Ketone bodies derived from fatty acid oxidation in the liver can penetrate the BBB by means of another transporter and can thus provide an alternative fuel for brain metabolism. Our initial experiences with the ketogenic diet in two adolescents and one adult are encouraging. Since the ketogenic diet has been used mainly in children and long-term effects in adults have not been established, careful follow-up of the patients is indicated.

Electronic database information

Accession numbers and URLs for data presented in this article are as follows:

Online Mendelian Inheritance in Man (OMIM), http://www.ncbi.nlm.nih.gov/Omim/
VIB Genetic Service Facility, http://www.vibgeneticservicefacility.be
NCBI, http://www.ncbi.nlm.nih.gov
ClustalW, http://www.ebi.ac.uk/clustalw/
Predictprotein, http://www.predictprotein.org

Supplementary material

Supplementary material is available at *Brain* online.

Acknowledgements

The authors are grateful to the family members for their kind cooperation and participation in this study. We acknowledge the contribution of the VIB Genetic Service Facility (http://www.vibgeneticservicefacility.be) to the genetic analyses. We thank Dr Mike Mueckler for providing the cDNA of *SLC2A1* (GLUT1). This research was funded by the Fund for Scientific Research Flanders (FWO-F), University of Antwerp and the Interuniversity Attraction Poles (IUAP) program P5/19 and P6/43 of the Belgian Science Policy Office (BELSPO). A.S. is a doctoral fellow of the University of Antwerp. L.D. is a PhD fellow of the Institute for Science and Technology (IWT), Belgium. H.V.E., L.R.F.C., K.G., W.V. and K.V.L. are funded by the Fund for Scientific Research Flanders (FWO-F), Belgium. Imaging studies were funded by the Interdisciplinary Research Program of the Research Fund of the K.U.Leuven (IDO/99/5 and IDO3/010). Functional studies in oocytes were funded by grants from the Federal Ministry for Education and Research in Germany (BMBF/NGFN2: 01GS0478) and by the European Union (Epicure: LSH 037315). H.L. is a Heisenberg fellow of the German Research Foundation (DFG).

References

Alderborn A, Kristofferson A, Hammerling U. Determination of single-nucleotide polymorphisms by real-time pyrophosphate DNA sequencing. Genome Res 2000; 10: 1249–58.

Auburger G, Ratzlaff T, Lunkes A, Nelles HW, Leube B, Binkofski F, et al. A gene for autosomal dominant paroxysmal choreoathetosis/spasticity (CSE) maps to the vicinity of a potassium channel gene cluster on chromosome 1p, probably within 2 cM between D1S443 and D1S197. Genomics 1996; 31: 90–4.

Berkovic SF. Paroxysmal movement disorders and epilepsy: links across the channel. Neurology 2000; 55: 169–70.

Bhatia KP, Soland VL, Bhatt MH, Quinn NP, Marsden CD. Paroxysmal exercise-induced dystonia: eight new sporadic cases and a review of the literature. Mov Disord 1997; 12: 1007–12.

Bing F, Dananchet Y, Vercueil L. [A family with exercise-induced paroxysmal dystonia and childhood absence epilepsy]. Rev Neurol (Paris) 2005; 161: 817–22.

Brockmann K, Dumitrescu AM, Best TT, Hanefeld F, Refetoff S. X-linked paroxysmal dyskinesia and severe global retardation caused by defective MCT8 gene. J Neurol 2005; 252: 663–6.

Brockmann K, Wang D, Korenke CG, von Moers A, Ho YY, Pascual JM, et al. Autosomal dominant glut-1 deficiency syndrome and familial epilepsy. Ann Neurol 2001; 50: 476–85.

Cottingham RW Jr, Idury RM, Schaffer AA. Faster sequential genetic linkage computations. Am J Hum Genet 1993; 53: 252–63.

Demirkiran M, Jankovic J. Paroxysmal dyskinesias: clinical features and classification. Ann Neurol 1995; 38: 571–9.

Deprez L, Peeters K, Van Paesschen W, Claeys KG, Claes LR, Suls A, et al. Familial occipitotemporal lobe epilepsy and migraine with visual aura: linkage to chromosome 9q. Neurology 2007; 68: 1995–2002.

De Vivo DC, Trifiletti RR, Jacobson RI, Ronen GM, Behmand RA, Harik SI. Defective glucose transport across the blood-brain barrier as a cause of persistent hypoglycorrhachia, seizures, and developmental delay. N Engl J Med 1991; 325: 703–9.

Du W, Bautista JF, Yang H, Diez-Sampedro A, You SA, Wang L, et al. Calcium-sensitive potassium channelopathy in human epilepsy and paroxysmal movement disorder. Nat Genet 2005; 37: 733–8.

Dupont P, Van Paesschen W, Palmini A, Ambayi R, Van Loon J, Goffin J, et al. Ictal perfusion patterns associated with single MRI-visible focal dysplastic lesions: implications for the noninvasive delineation of the epileptogenic zone. Epilepsia 2006; 47: 1550–7.

Friedman JR, Thiele EA, Wang D, Levine KB, Cloherty EK, Pfeifer HH, et al. Atypical GLUT1 deficiency with prominent movement disorder responsive to ketogenic diet. Mov Disord 2006; 21: 241–5.

Guerrini R, Bonanni P, Nardocci N, Parmeggiani L, Piccirilli M, De Fusco M, et al. Autosomal recessive rolandic epilepsy with paroxysmal exercise-induced dystonia and writer's cramp: delineation of the syndrome and gene mapping to chromosome 16p12-11.2. Ann Neurol 1999; 45: 344–52.

Guerrini R, Sanchez-Carpintero R, Deonna T, Santucci M, Bhatia KP, Moreno T, et al. Early-onset absence epilepsy and paroxysmal dyskinesia. Epilepsia 2002; 43: 1224–9.

Ho YY, Wang D, Hinton V, Yang H, Vasilescu A, Engelstad K, et al. Glut-1 deficiency syndrome: autosomal dominant transmission of the R126C Missense mutation. Ann Neurol 2001; 50: S125.

Iserovich P, Wang D, Ma L, Yang H, Zuniga FA, Pascual JM, et al. Changes in glucose transport and water permeability resulting from the T310I pathogenic mutation in Glut1 are consistent with two transport channels per monomer. J Biol Chem 2002; 277: 30991–7.

Jankovic J, Demirkiran M. Paroxysmal dyskinesias: an update. Ann Med Sci 2001; 10: 92–103.

Kamm C, Mayer P, Sharma M, Niemann G, Gasser T. New family with paroxysmal exercise-induced dystonia and epilepsy. Mov Disord 2007; 22: 873–7.

Kato N, Sadamatsu M, Kikuchi T, Niikawa N, Fukuyama Y. Paroxysmal kinesigenic choreoathetosis: from first discovery in 1892 to genetic

linkage with benign familial infantile convulsions. Epilepsy Res 2006; 70 (Suppl 1): S174–84.

Kikuchi T, Nomura M, Tomita H, Harada N, Kanai K, Konishi T, et al. Paroxysmal kinesigenic choreoathetosis (PKC): confirmation of linkage to 16p11-q21, but unsuccessful detection of mutations among 157 genes at the PKC-critical region in seven PKC families. J Hum Genet 2007; 52: 334–41.

Klepper J, Diefenbach S, Kohlschutter A, Voit T. Effects of the ketogenic diet in the glucose transporter 1 deficiency syndrome. Prostaglandins Leukot Essent Fatty Acids 2004; 70: 321–7.

Klepper J, Leiendecker B. GLUT1 deficiency syndrome-2007 update. Dev Med Child Neurol 2007; 49: 707–16.

Klepper J, Monden I, Guertsen E, Voit T, Willemsen M, Keller K. Functional consequences of the autosomal dominant G272A mutation in the human GLUT1 gene. FEBS Lett 2001a; 498: 104–9.

Klepper J, Salas-Burgos A, Gertsen E, Fischbarg J. Bench meets bedside: a 10-year-old girl and amino acid residue glycine 75 of the facilitative glucose transporter GLUT1. Biochemistry 2005; 44: 12621–6.

Klepper J, Willemsen M, Verrips A, Guertsen E, Herrmann R, Kutzick C, et al. Autosomal dominant transmission of GLUT1 deficiency. Hum Mol Genet 2001b; 10: 63–8.

Kluge A, Kettner B, Zschenderlein R, Sandrock D, Munz DL, Hesse S, et al. Changes in perfusion pattern using ECD-SPECT indicate frontal lobe and cerebellar involvement in exercise-induced paroxysmal dystonia. Mov Disord 1998; 13: 125–34.

Lance JW. Familial paroxysmal dystonic choreoathetosis of Mount and Reback and its differentiation from related syndromes. Trans Am Neurol Assoc 1977; 102: 46–8.

Leary LD, Wang D, Nordli DR Jr, Engelstad K, De Vivo DC. Seizure characterization and electroencephalographic features in Glut-1 deficiency syndrome. Epilepsia 2003; 44: 701–7.

Lee WL, Tay A, Ong HT, Goh LM, Monaco AP, Szepetowski P. Association of infantile convulsions with paroxysmal dyskinesias (ICCA syndrome): confirmation of linkage to human chromosome 16p12-q12 in a Chinese family. Hum Genet 1998; 103: 608–12.

Margari L, Perniola T, Illiceto G, Ferrannini E, De Iaco MG, Presicci A, et al. Familial paroxysmal exercise-induced dyskinesia and benign epilepsy: a clinical and neurophysiological study of an uncommon disorder. Neurol Sci 2000; 21: 165–72.

Mueckler M, Caruso C, Baldwin SA, Panico M, Blench I, Morris HR, et al. Sequence and structure of a human glucose transporter. Science 1985; 229: 941–5.

Munchau A, Valente EM, Shahidi GA, Eunson LH, Hanna MG, Quinn NP, et al. A new family with paroxysmal exercise induced dystonia and migraine: a clinical and genetic study. J Neurol Neurosurg Psychiatry 2000; 68: 609–14.

Nagamitsu S, Matsuishi T, Hashimoto K, Yamashita Y, Aihara M, Shimizu K, et al. Multicenter study of paroxysmal dyskinesias in Japan–clinical and pedigree analysis. Mov Disord 1999; 14: 658–63.

Nardocci N, Lamperti E, Rumi V, Angelini L. Typical and atypical forms of paroxysmal choreoathetosis. Dev Med Child Neurol 1989; 31: 670–4.

Neville BG, Besag FM, Marsden CD. Exercise induced steroid dependent dystonia, ataxia, and alternating hemiplegia associated with epilepsy. J Neurol Neurosurg Psychiatry 1998; 65: 241–4.

Overweg-Plandsoen WC, Groener JE, Wang D, Onkenhout W, Brouwer OF, Bakker HD, et al. GLUT-1 deficiency without epilepsy–an exceptional case. J Inherit Metab Dis 2003; 26: 559–63.

Pascual JM, Van Heertum RL, Wang D, Engelstad K, De Vivo DC. Imaging the metabolic footprint of Glut1 deficiency on the brain. Ann Neurol 2002; 52: 458–64.

Plant GT, Williams AC, Earl CJ, Marsden CD. Familial paroxysmal dystonia induced by exercise. J Neurol Neurosurg Psychiatry 1984; 47: 275–9.

Rainier S, Thomas D, Tokarz D, Ming L, Bui M, Plein E, et al. Myofibrillogenesis regulator 1 gene mutations cause paroxysmal dystonic choreoathetosis. Arch Neurol 2004; 61: 1025–9.

Signorini M, Paulesu E, Friston K, Perani D, Colleluori A, Lucignani G, et al. Rapid assessment of regional cerebral metabolic abnormalities in single subjects with quantitative and nonquantitative [18F]FDG PET: a clinical validation of statistical parametric mapping. Neuroimage 1999; 9: 63–80.

Swoboda KJ, Soong B, McKenna C, Brunt ER, Litt M, Bale JF Jr, et al. Paroxysmal kinesigenic dyskinesia and infantile convulsions: clinical and linkage studies. Neurology 2000; 55: 224–30.

Szepetowski P, Rochette J, Berquin P, Piussan C, Lathrop GM, Monaco AP. Familial infantile convulsions and paroxysmal choreoathetosis: a new neurological syndrome linked to the pericentromeric region of human chromosome 16. Am J Hum Genet 1997; 61: 889–98.

Van Laere K, Nuttin B, Gabriels L, Dupont P, Rasmussen S, Greenberg BD, et al. Metabolic imaging of anterior capsular stimulation in refractory obsessive-compulsive disorder: a key role for the subgenual anterior cingulate and ventral striatum. J Nucl Med 2006; 47: 740–7.

Wali GM. Paroxysmal hemidystonia induced by prolonged exercise and cold. J Neurol Neurosurg Psychiatry 1992; 55: 236–7.

Wang D, Pascual JM, Iserovich P, Yang H, Ma L, Kuang K, et al. Functional studies of threonine 310 mutations in Glut1: T310I is pathogenic, causing Glut1 deficiency. J Biol Chem 2003; 278: 49015–21.

Wang D, Pascual JM, Yang H, Engelstad K, Jhung S, Sun RP, et al. Glut-1 deficiency syndrome: clinical, genetic, and therapeutic aspects. Ann Neurol 2005; 57: 111–8.

Weber YG, Storch A, Wuttke TV, Brockmann K, Kempfle J, Maljevic S, et al. GLUT1 mutations are a cause of paroxysmal exertion-induced dyskinesias and induce hemolytic anemia by a cation leak. J Clin Invest 2008; 118: 2157–68.

Weckx S, Del Favero J, Rademakers R, Claes L, Cruts M, De Jonghe P, et al. novoSNP, a novel computational tool for sequence variation discovery. Genome Res 2005; 15: 436–42.

Wong HY, Law PY, Ho YY. Disease-associated Glut1 single amino acid substitute mutations S66F, R126C, and T295M constitute Glut1-deficiency states in vitro. Mol Genet Metab 2007; 90: 193–8.